Examining the Callaway model for lattice thermal conductivity

Jinlong Ma,[1] Wu Li,[2,*] and Xiaobing Luo[1,†]

[1]*School of Energy and Power Engineering, Huazhong University of Science and Technology, Wuhan 430074, China*

[2]*Scientific Computing & Modelling NV, De Boelelaan 1083, 1081 HV Amsterdam, The Netherlands*

(Received 22 April 2014; revised manuscript received 5 June 2014; published 14 July 2014)

The Callaway model [J. Callaway, Phys. Rev. **113**, 1046 (1959)], regarded as an improvement over the relaxation time approximation (RTA) for the phonon Boltzmann transport equation (BTE), is widely used in studying lattice thermal conductivity (κ). However, its accuracy needs to be systematically examined. By solving BTE accurately using an iterative method along with the first principles calculation of phonon scatterings, we conduct such an examination of the Callaway model as well as a modified version proposed by Allen [Phys. Rev. B **88**, 144302 (2013)] for Si, diamond, and wurtzite AlN. At room temperature, the RTA underestimates κ by 5%, 32%, 11%, and 12% for Si, diamond, and in-plane and cross-plane AlN, respectively. The deviation of the original Callaway model from the accurate κ is −1%, 25%, 1%, and −12%, respectively, while the deviation of Allen's modified model is 7%, 44%, 13%, and −8%, respectively. The room temperature anisotropy of AlN is 5%, and the anisotropy predicted by RTA, the Callaway model, and Allen's modified version is 7%, 19%, and 29%, respectively. We conclude that neither the original Callaway model nor Allen's modified version can generally guarantee an improvement over RTA. In these three systems, we also find that the relaxation times for umklapp processes scale as $1/\omega^3$ at low frequencies for both transverse acoustic (TA) and longitudinal acoustic (LA) modes, and those for normal processes scale as $1/\omega$ and $1/\omega^2$ for TA and LA modes, respectively.

DOI: 10.1103/PhysRevB.90.035203 PACS number(s): 44.10.+i

I. INTRODUCTION

The phonon Boltzmann transport equation [1,2] (BTE) is a frequently used approach to study the lattice thermal conductivity (κ). Its linearized version is simply a set of linear equations. Since the linear-equation set has a large dimension, the BTE is far from trivial to solve. On the other hand, the lack of reliable linear coefficients determined by the interatomic potential can also make the exact solution of BTE not so necessary. Instead, the relaxation time approximation (RTA) for BTE, along with the Debye approximation neglecting phonon dispersion, was conventionally employed, and several parameters were introduced to treat different scattering mechanisms. The phonon wave-vector conservative normal (N) processes alone should lead to zero resistance [1,2], and thus the normal processes can play a different role from the wave-vector nonconservative umklapp (U) processes. However, they are treated equally in RTA. Callaway proposed an intuitive model to treat N processes and U processes differently [3]. Since then it has been widely used [4–31]. However, the accuracy of Callaway model was not known. Very recently, a modified Callaway model has been proposed by Allen, which uses a different constraint condition imposed by the N processes [32].

In 1995 a practically feasible, iterative numerical method was proposed [33–35] to accurately solve BTE. A first principles determination of the interatomic force constants (IFCs) has been developed recently, which enables the *ab initio* calculations of κ. So far, this method has been applied to many systems such as Si and Ge [36–39], diamond [40–43], MgO [44], Si_xGe_{1-x} [45–47], half-Heusler compounds [48,49], PbSe, PbTe, and $PbSe_xTe_{1-x}$ alloys [50], Ga-V compounds [51–53], Mg_2Si, Mg_2Sn, and $Mg_2Si_xSn_{1-x}$ alloys [54], In-V compounds [53], Al-V compounds [53,55], SiC [53], BeO [55], $MgSiO_3$ [56], UO_2 [57], B-V compounds [58], and skutterudites [59], showing good agreement with available experimental data. Some of the authors and their co-workers have recently published an open-source code ShengBTE [60], which allows one to calculate the third-order IFCs using a real-space finite-difference approach [54,60] along with third-party *ab initio* packages and eventually κ using a locally adaptive algorithm to treat the Gaussian function approximation for the Dirac delta function [41,60]. The accurate solution scheme of BTE combined with the first principles determination of the linear coefficients in BTE makes it possible to examine the Callaway model based on real systems. Ward *et al.* [37] made such an examination for Si and they found that the Callaway model agrees well with the precise solution. Despite that, a systematic examination is still lacking.

In this paper, we conduct such an examination of the accuracy of the original Callaway model and Allen's modified version with three systems, Si, diamond, and wurtzite AlN. We find that neither of these two approximations has a guaranteed accuracy and improvement over RTA. Though RTA generally underestimates κ, the Callaway model and Allen's modified model can either underestimate or overestimate κ.

II. PHONON BOLTZMANN TRANSPORT EQUATION

A. Linearized phonon BTE

In the presence of a temperature gradient ∇T, the phonon distribution function f_λ in crystals deviates from the equilibrium Bose-Einstein distribution f_λ^0, and this deviation can be obtained from the phonon BTE [54,60],

$$-\mathbf{v}_\lambda \cdot \nabla T \frac{\partial f_\lambda}{\partial T} + \left.\frac{\partial f_\lambda}{\partial t}\right|_{\text{scatt}} = 0, \quad (1)$$

*wu.li.phys2011@gmail.com

†luoxb@hust.edu.cn

where λ denotes a phonon mode comprising a wave vector $\mathbf{q}$ and a phonon branch p. $\mathbf{v}_\lambda$ is the phonon group velocity. The first term in the equation is the diffusion term due to the temperature gradient, and the second term is the scattering term determined by the scattering events occurring in the system. For a small temperature gradient, the phonon BTE can be linearized with $f_\lambda = f_\lambda^0 + f_\lambda^0(1+f_\lambda^0)\Phi_\lambda$, where Φ_λ is a small perturbation. If only three-phonon processes are considered in the scattering term, the linearized phonon BTE can be written as [61,62]

$$-\mathbf{v}_\lambda\cdot\nabla T\frac{\partial f_\lambda^0}{\partial T} = \frac{f_\lambda^0(1+f_\lambda^0)}{N} \times\sum_{\lambda'\lambda''}\Big[(\Phi_\lambda+\Phi_{\lambda'}-\Phi_{\lambda''})\Gamma^+_{\lambda\lambda'\lambda''} +\frac{1}{2}(\Phi_\lambda-\Phi_{\lambda'}-\Phi_{\lambda''})\Gamma^-_{\lambda\lambda'\lambda''}\Big], \quad (2)$$

where we introduce a discretization of the Brillouin zone (BZ) into a Gamma-point-centered regular grid of $N = N_1\times N_2\times N_3$ $\mathbf{q}$ points. $\Gamma^\pm_{\lambda\lambda'\lambda''}$ are related to transition rates for three-phonon absorption (+) and emission (−) processes, which can be computed successfully by first principles [36,40,42,51,54]. In absorption processes a phonon λ is scattered by absorbing a phonon λ' to yield a third phonon λ'', while in emission processes a phonon λ decays into two phonons λ' and λ''. All the allowed three-phonon processes must conserve both energy ($\omega_\lambda \pm \omega'_\lambda = \omega''_\lambda$) and momentum ($\mathbf{q}_\lambda \pm \mathbf{q}'_\lambda = \mathbf{q}''_\lambda + \mathbf{G}$), where + and − are for absorption and emission processes, respectively, and $\mathbf{G}$ is a reciprocal lattice vector such that $\mathbf{q}$, $\mathbf{q}'$, and $\mathbf{q}''$ are in the same image of the BZ. If $\mathbf{G}=\mathbf{0}$, the processes are N processes, and if not, they are U processes. The distinction between the N processes and U processes is not rigorous, since it depends on the choice of the BZ image. Some U processes in one BZ image might be described as N processes in another BZ image. Conventionally all $\mathbf{q}$ points are restricted to the first BZ, that is, the Wigner-Seitz cell, since the direction of the phonon group velocity is closer to the direction of $\mathbf{q}$ in this case.

Since Φ_λ is linear with ∇T, we write $\Phi_\lambda = -\frac{\hbar\omega_\lambda}{k_B T^2}\mathbf{F}_\lambda\cdot\nabla T$, where $\mathbf{F}_\lambda$ can be regarded as mean free displacement, a generalization of mean free path [60], and ω_λ is the angular frequency. To simplify Eq. (2), we further define $\mathbf{E}_\lambda \equiv \omega_\lambda\mathbf{F}_\lambda$, and we can obtain

$$\Big\{-\omega_\lambda\mathbf{v}_\lambda+\frac{1}{N}\sum_{\lambda'\lambda''}\Big[(\mathbf{E}_\lambda+\mathbf{E}_{\lambda'}-\mathbf{E}_{\lambda''})\Gamma^+_{\lambda\lambda'\lambda''} +\frac{1}{2}(\mathbf{E}_\lambda-\mathbf{E}_{\lambda'}-\mathbf{E}_{\lambda''})\Gamma^-_{\lambda\lambda'\lambda''}\Big]\Big\}\cdot\nabla T = 0. \quad (3)$$

Equating the contents of the curly brackets to zero, one can see that the phonon BTE can be viewed as a set of linear equations in terms of $\mathbf{E}_\lambda$ in the form of $\sum_{\lambda'} A_{\lambda\lambda'}\mathbf{E}_{\lambda'} = \mathbf{B}_\lambda$, where A is the coefficient square matrix and $\mathbf{B}_\lambda = \omega_\lambda\mathbf{v}_\lambda$. When only N processes exist, it is obvious that the $\sum_{\lambda'} A_{\lambda\lambda'}\mathbf{E}_{\lambda'} = \mathbf{0}$ is valid not only for $\mathbf{E}_{\lambda'}=\mathbf{0}$ but also for $\mathbf{E}_{\lambda'}=\mathbf{q}_{\lambda'}$. This indicates that a nonzero current can be present in the case of vanishing ∇T. Therefore, N processes alone lead to an infinite κ. Mathematically it corresponds to a case where A is a singular matrix and the solution of $\sum_{\lambda'} A_{\lambda\lambda'}\mathbf{E}_{\lambda'} = \mathbf{B}_\lambda$ is principally infinite. Even though κ is infinite in this case, it is too rude to say that N processes are nonresistive and U processes are resistive. As was mentioned above, the distinction between N processes and U processes depends on the BZ scheme that is referred to. Additionally, the fact that N processes alone result in an infinite κ is not restricted to any particular choice of BZ.

The heat current $\mathbf{J}$ generated from the small temperature gradient can be expressed in terms of the distribution function [32,62],

$$\mathbf{J} = \frac{1}{NV}\sum_\lambda \hbar\omega_\lambda\mathbf{v}_\lambda f_\lambda = -\frac{1}{k_B T^2 NV}\sum_\lambda \hbar^2\omega_\lambda f_\lambda^0(1+f_\lambda^0)\mathbf{v}_\lambda(\mathbf{E}_\lambda\cdot\nabla T), \quad (4)$$

where V is the volume of the unit cell and we have used the fact the heat current is vanishing at the equilibrium state. From Fourier's law $J^\alpha = -\sum_\beta \kappa^{\alpha\beta}(\nabla T)^\beta$, it follows

$$\kappa^{\alpha\beta} = \frac{1}{k_B T^2 NV}\sum_\lambda \hbar^2\omega_\lambda f_\lambda^0(1+f_\lambda^0)v_\lambda^\alpha E_\lambda^\beta. \quad (5)$$

B. Callaway model

It is far from trivial to solve the linear equations $\sum_{\lambda'} A_{\lambda\lambda'}\mathbf{E}_{\lambda'} = \mathbf{B}_\lambda$, since a large dimension is involved. On the other hand, the lack of reliable linear coefficients $A_{\lambda\lambda'}$ determined by the interatomic potential can also make the exact solution of BTE not so necessary. Instead RTA is often used,

$$-\mathbf{v}_\lambda\cdot\nabla T\frac{\partial f_\lambda^0}{\partial T} = \frac{f_\lambda - f_\lambda^0}{\tau_\lambda^c}, \quad (6)$$

where the relaxation time τ_λ^c is usually parametrized. RTA always underestimates κ, since not all scattering processes are completely resistive. For instance, it gives a finite κ in the case of N processes alone. Thus, Callaway treated N processes and U processes separately, $1/\tau_\lambda^c = 1/\tau_\lambda^N + 1/\tau_\lambda^U$, where τ_λ^N and τ_λ^U are relaxation times for N processes and U processes, respectively, and replaced Eq. (6) with [3,32]

$$-\mathbf{v}_\lambda\cdot\nabla T\frac{\partial f_\lambda^0}{\partial T} = \frac{f_\lambda - f_\lambda^0}{\tau_\lambda^U} + \frac{f_\lambda - f_\lambda^*}{\tau_\lambda^N}. \quad (7)$$

While the U processes tend to relax the phonon distribution to equilibrium distribution f_λ^0, the N processes drag it to a displaced distribution f_λ^* depending on $\mathbf{q}_\lambda$ as well as ω_λ. The displaced distribution function can be written as [3,32]

$$f_\lambda^* = \frac{1}{e^{\hbar\omega_\lambda/k_B T+\mathbf{\Lambda}\cdot\mathbf{q}_\lambda}-1} \approx f_\lambda^0 - f_\lambda^0(1+f_\lambda^0)\mathbf{\Lambda}\cdot\mathbf{q}_\lambda, \quad (8)$$

where $\mathbf{\Lambda}$ is a Lagrange multiplier. Substituting Eq. (8) into Eq. (7), we can obtain

$$f_\lambda - f_\lambda^0 = -\tau_\lambda^c\mathbf{v}_\lambda\cdot\nabla T\frac{\partial f_\lambda^0}{\partial T} - \frac{\tau_\lambda^c}{\tau_\lambda^N}\frac{k_B T^2}{\hbar\omega_\lambda}\mathbf{\Lambda}\cdot\mathbf{q}_\lambda\frac{\partial f_\lambda^0}{\partial T}. \quad (9)$$

To solve $\mathbf{\Lambda}$, Callaway utilized the fact that the N processes conserve phonon momentum. The rate of change of the total

phonon momentum due to N processes is set equal to zero [3],

$$\sum_{\lambda} \frac{f_{\lambda} - f_{\lambda}^{*}}{\tau_{\lambda}^{N}} \cdot \mathbf{q}_{\lambda} = \mathbf{0}. \tag{10}$$

Inserting Eqs. (8) and (9) into Eq. (10), one can obtain

$$\sum_{\lambda} \frac{\tau_{\lambda}^{c}}{\tau_{\lambda}^{N}} (\mathbf{v}_{\lambda} \cdot \nabla T) \mathbf{q}_{\lambda} \frac{\partial f_{\lambda}^{0}}{\partial T} = \sum_{\lambda} \frac{\tau_{\lambda}^{c}}{\tau_{\lambda}^{N} \tau_{\lambda}^{U}} \frac{k_B T^2}{\hbar \omega_{\lambda}} (\mathbf{\Lambda} \cdot \mathbf{q}_{\lambda}) \mathbf{q}_{\lambda} \frac{\partial f_{\lambda}^{0}}{\partial T}. \tag{11}$$

Though $\mathbf{\Lambda}$ is linear with ∇T, it does not necessarily orient along the same direction. Lattice symmetry imposes a constraint on the relation of its directions. For instance, in the case of a cubic lattice or ∇T in the plane or perpendicular to the plane of a wurtzite lattice, as considered in this paper, $\mathbf{\Lambda}$ as well as $\mathbf{J}$ are parallel to ∇T. The solution of $\mathbf{\Lambda}$ simplifies in these cases. Assuming the thermal gradient is along the α direction, only Λ_{α} is not vanishing, and can be obtained as

$$\frac{\Lambda_{\alpha}}{\nabla_{\alpha} T} = \frac{1}{k_B T^2} \frac{\sum_{\lambda} \hbar \omega_{\lambda} \tau_{\lambda}^{c} \left(\tau_{\lambda}^{N}\right)^{-1} v_{\lambda}^{\alpha} q_{\lambda}^{\alpha} f_{\lambda}^{0} \left(1 + f_{\lambda}^{0}\right)}{\sum_{\lambda} \tau_{\lambda}^{c} \left(\tau_{\lambda}^{N} \tau_{\lambda}^{U}\right)^{-1} q_{\lambda}^{\alpha} q_{\lambda}^{\alpha} f_{\lambda}^{0} \left(1 + f_{\lambda}^{0}\right)}. \tag{12}$$

Then combining the solution of Λ_{α} [Eq. (12)] and the distribution f_{λ} [Eq. (9)], the heat current can be obtained with Eq. (4), thus the κ calculated from Callaway's approximated phonon BTE can be expressed as

$$\kappa^{\alpha\alpha} = \kappa_{\mathrm{RTA}}^{\alpha\alpha} + \frac{I_1^{\alpha} I_2^{\alpha}}{I_3^{\alpha}}, \tag{13}$$

where

$$\kappa_{\mathrm{RTA}}^{\alpha\alpha} = \frac{1}{k_B T^2 N V} \sum_{\lambda} (\hbar \omega_{\lambda})^2 v_{\lambda}^{\alpha} v_{\lambda}^{\alpha} \tau_{\lambda}^{c} f_{\lambda}^{0} \left(1 + f_{\lambda}^{0}\right), \tag{14}$$

corresponding to the κ obtained from the ordinary RTA [Eq. (6)], and the correction terms can be expressed as

$$I_1^{\alpha} = I_2^{\alpha} = \frac{1}{k_B T^2 N V} \sum_{\lambda} \frac{\tau_{\lambda}^{c}}{\tau_{\lambda}^{N}} \hbar \omega_{\lambda} v_{\lambda}^{\alpha} q_{\lambda}^{\alpha} f_{\lambda}^{0} \left(1 + f_{\lambda}^{0}\right), \tag{15a}$$

$$I_3^{\alpha} = \frac{1}{k_B T^2 N V} \sum_{\lambda} \frac{\tau_{\lambda}^{c}}{\tau_{\lambda}^{N} \tau_{\lambda}^{U}} q_{\lambda}^{\alpha} q_{\lambda}^{\alpha} f_{\lambda}^{0} \left(1 + f_{\lambda}^{0}\right). \tag{15b}$$

Very recently, Allen [32] proposed a different constraint equation for $\mathbf{\Lambda}$, which claims the total phonon momentum should be the same for both the actual distribution and the displaced equilibrium distribution:

$$\sum_{\lambda} (f_{\lambda} - f_{\lambda}^{*}) \cdot \mathbf{q}_{\lambda} = \mathbf{0}. \tag{16}$$

This avoids the extra use of the RTA, and consequently the factor $1/\tau_{\lambda}^{N}$ is removed from the sums in the linear equation for $\mathbf{\Lambda}$ [Eq. (11)] as well as I_1 [Eq. (15a)] and I_3 [Eq. (15b)] for the correction to $\kappa_{\mathrm{RTA}}^{\alpha\alpha}$. I_2 [Eq. (15a)] for the correction remains the same. Allen [32] showed his modified Callaway model can lead to higher κ by using simple parametrization for τ_{λ}^{N} and τ_{λ}^{U}.

C. Iterative BTE

Owing to the recent development of techniques calculating the IFCs from first principles, the transition rates $\Gamma_{\lambda\lambda'\lambda''}^{\pm}$ can be obtained accurately. Then the direct solution of linear equations $\sum_{\lambda'} A_{\lambda\lambda'} \mathbf{E}_{\lambda'} = \mathbf{B}_{\lambda}$ involved in Eq. (3) enables accurate determination of κ. It is efficient to employ an iteration solution. Pulling $\mathbf{E}_{\lambda}$ out of summation term in Eq. (3), one obtains its iterative form as

$$\mathbf{E}_{\lambda}^{i+1} = \mathbf{E}_{\lambda}^{0} + \frac{\tau_{\lambda}^{0}}{N} \sum_{\lambda'\lambda''} \left[\left(\mathbf{E}_{\lambda''}^{i} - \mathbf{E}_{\lambda'}^{i}\right) \Gamma_{\lambda\lambda'\lambda''}^{+} + \frac{1}{2} \left(\mathbf{E}_{\lambda''}^{i} + \mathbf{E}_{\lambda'}^{i}\right) \Gamma_{\lambda\lambda'\lambda''}^{-} \right], \quad i = 1,2,3,\ldots. \tag{17}$$

The iterative process is started with

$$\mathbf{E}_{\lambda}^{0} = \omega_{\lambda} \mathbf{v}_{\lambda} \tau_{\lambda}^{0}, \tag{18}$$

with $\frac{1}{\tau_{\lambda}^{0}} = \frac{1}{N} \sum_{\lambda'\lambda''} [\Gamma_{\lambda\lambda'\lambda''}^{+} + \frac{1}{2} \Gamma_{\lambda\lambda'\lambda''}^{-}]$. τ_{λ}^{c} used in Eq. (6) is equal to τ_{λ}^{0} principally. In fact, setting E_{λ} equal to E_{λ}^{0} is equivalent to RTA [60]. τ_{λ}^{N} and τ_{λ}^{U} used in last section can also be obtained accurately, as long as N processes and U processes are separated.

Once the difference between the values of $\mathbf{E}_{\lambda}$ in two consecutive steps is below a specified accuracy level, the iteration scheme is terminated. Strictly speaking, the $\mathbf{E}_{\lambda}$ should converge for all phonon modes in the iterative process. However, the convergency of $\mathbf{E}_{\lambda}$ is too slow numerically. Instead, a natural choice of the convergence criterion for κ is implemented [60]. A test of this choice using a relatively small $24 \times 24 \times 24$ mesh for Si shows that this iterative solution of phonon BTE gives exactly the same κ as that obtained by using LU decomposition algorithm to solve the linear equations $\sum_{\lambda'} A_{\lambda\lambda'} \mathbf{E}_{\lambda'} = \mathbf{B}_{\lambda}$.

III. RESULTS AND DISCUSSION

In this section we calculate the transition rates and relaxation times from IFCs determined from first principles [41,55] and examine the accuracy of the Callaway model and Allen's modified model for Si, diamond, and wurtzite AlN. Previous calculations [37,40,53] show that at room temperature the full solution of BTE corrects RTA only by 6% for Si, and by 33% for diamond, which is the largest among all the bulk systems that have been studied in the literature. The correction for wurtzite AlN [55] is somewhere in between Si and diamond. κ of cubic systems such as Si and diamond reduces to a scalar, and the anisotropy of κ of AlN, characterized by the difference between the in-plane and cross-plane values, provides another degree of freedom to check the accuracy.

A. Si

The intrinsic κ calculated using different methods to solving phonon BTE for Si between 50 and 500 K are shown in Fig. 1. The calculated room temperature κ of RTA and exactly iterative solution are respectively 146 and 153 W m^{-1} K^{-1}, which agree with previous works [37,41,53]. Above 100 K, comparing the RTA κ and its accurate values, we find that the underestimation of RTA is very small, only about 5%. Inserting the calculated *ab initio* intrinsic relaxation times into the original Callaway model, it shows satisfactory agreement with the exact *ab initio* results, with the largest deviation below 2%. At room temperature, the underestimation is only 1%. When using Allen's modified model to conduct the correction, it gives

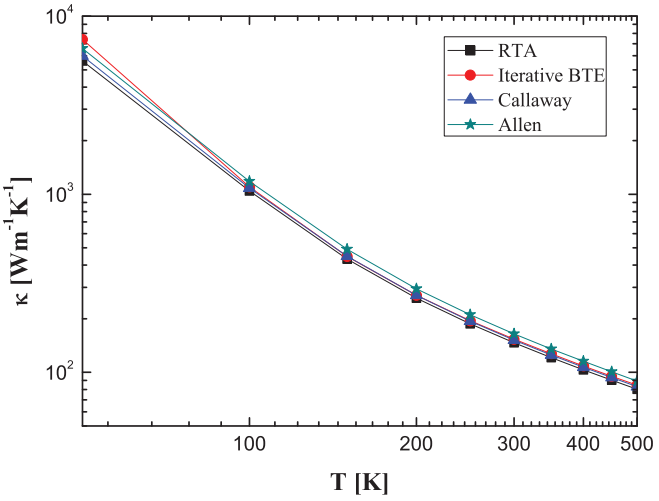

FIG. 1. (Color online) Thermal conductivity of Si calculated with different methods for solving phonon BTE, as a function of temperature. The square line (RTA) is the result of RTA solution, the circle line (iterative BTE) is the result of iterative solution, the triangle line (Callaway) is the result of the Callaway model, and the star line (Allen) is the result of Allen's modified model.

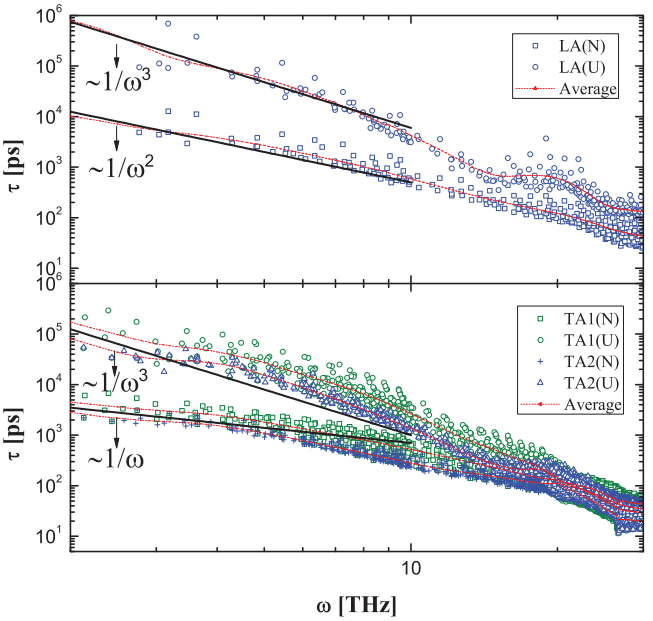

FIG. 2. (Color online) Relaxation time of N processes and U processes in Si at 300 K, as a function of frequency. The top panel is for the LA branch and the bottom panel is for the lowest TA (TA1) and second lowest TA (TA2) branches. The discrete data are *ab initio* results, the dashed lines are the averaged relaxation times, and the solid lines are fitting lines.

a larger κ than the original Callaway model and overestimates κ obviously. For instance, it overestimates κ by about 7% at 300 K. At 50 K, the RTA gives about 24% underestimation, and both the original Callaway model and Allen's modified model underestimate κ by 19% and 11%, respectively. This demonstrates that neither the original Callaway model nor Allen's modified model has guaranteed accuracy, though the original Callaway model performs better than the ordinary RTA in the case of Si.

It is interesting to compare the relaxation times with previous work. Ward and Broido [37] reported that for the longitudinal acoustic (LA) branch τ^U exhibits a $1/\omega^4$ frequency dependence, which is different from the often assumed $1/\omega^2$ frequency dependence. τ^N of the LA branch is found to follow well $1/\omega^2$ [37]. Later, Esfarjani *et al.* [38] showed although τ^N scales as $1/\omega^2$, τ^U scales as $1/\omega^3$ at low frequencies. However, there is no distinction between LA and transverse acoustic (TA) and only a $18 \times 18 \times 18$ mesh was used in their work, leading to an insufficient number of data points at low frequencies [38]. Actually, Herring [63] predicted different behavior for the LA and TA branches. According to his work, for Si, τ of the LA and TA branches should scale as $1/\omega^2$ and $1/\omega$, respectively. We use a $105 \times 105 \times 105$ mesh of grid $\mathbf{q}$ sampling to calculate the relaxation time for $\omega < 10$ THz, and a $60 \times 60 \times 60$ mesh for 10–30 THz. The results are converged for $\omega > 2$ THz and plotted in Fig. 2 for the two TA branches and the LA branch. In order to analyze the data more easily, we average the relaxation times by using $\bar{\tau}(\omega) = \sum_\lambda \tau_\lambda \delta(\omega - \omega_\lambda) / \sum_\lambda \delta(\omega - \omega_\lambda)$. The δ function is approximated with Gaussian function $\delta(\omega - \omega_\lambda) \approx \frac{1}{\sqrt{2\pi}\sigma} e^{-(\omega-\omega_\lambda)^2/2\sigma^2}$, where σ is the adaptive broadening parameter depending on the mode group velocity [41,60]. As can be seen in Fig. 2, τ^U scales as $1/\omega^3$ at low frequencies for all three acoustic branches, which can agree with the work by Esfarjani *et al.* [38]. τ^N apparently has a $1/\omega^2$ dependence for the LA branch. For TA branches τ^N scales as $1/\omega$ at low frequencies, and it tends to have a stronger frequency dependence such as $1/\omega^2$ at higher frequencies. Therefore, the $1/\omega^2$ behavior established by Esfarjani *et al.* [38] is likely because the frequencies are not low enough. The different frequency dependence for the LA and TA branches revealed in our calculation agrees with Herring's prediction [63]. The dominant $1/\omega$ dependence for the TA branches is independent of the lattice symmetry, and results from the three-phonon processes TA + LA → LA, where the two LA modes are not in the neighborhood of any degeneracy points. The frequency dependence of τ for the LA branch is determined by the degeneracy of the phonon frequencies due to the point group symmetries of the lattice [63]. The relaxation time for the LA branch scales as $1/\omega^2$ for high symmetry crystals, while it is $1/\omega^3$ and perhaps sometimes $1/\omega^4$ for those with lower symmetry. To be specific, in cubic crystals, the relaxation time for the LA branch scales as $1/\omega^2$ if the point group is O_h, which Si belongs to, or the T_d point group. However, it follows $1/\omega^3$ in the case of T_h while $1/\omega^4$ for the O and T point groups. Additionally, the relaxation times show the same power-law frequency dependence at 100 K, which is not shown here.

B. Diamond

Figure 3 shows the κ from different solutions for diamond ranging from 100 to 500 K. It can be seen that the full solution of phonon BTE gives a much higher κ than the RTA, for instance, about 32% larger at room temperature. As mentioned above, the underestimation of RTA is due to the equally resistive treatment of the N processes, which become

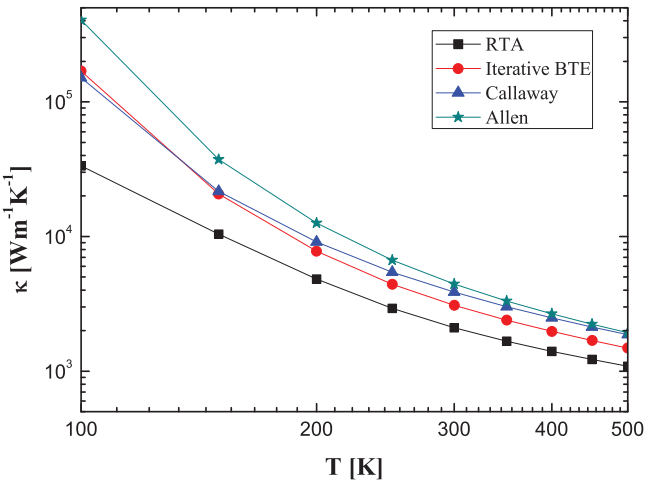

FIG. 3. (Color online) Thermal conductivity of diamond calculated with different methods for solving phonon BTE, as a function of temperature.

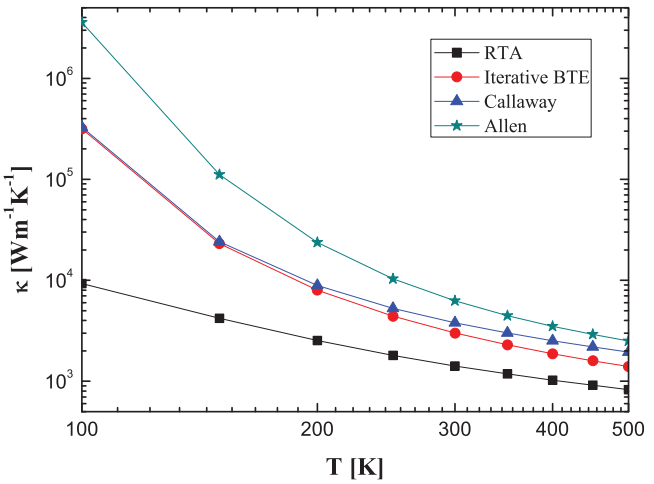

FIG. 4. (Color online) Thermal conductivity of a diamond-based system calculated with linear phonon dispersions and approximated three-phonon relaxation times derived from a long wavelength approximation, as a function of temperature.

stronger at lower temperature. Thus, the underestimation becomes larger as the temperature decreases, varying from 27% at 500 K to 80% at 100 K. The corrections to RTA decrease with increasing temperature, because the portion of N processes becomes less. As a result, the difference between the original Callaway model and Allen's model decreases as well. The original Callaway model agrees with the iterative solution better at lower temperature where N processes are more important, which is in contrast to the Si case. Allen's modified model predicts a larger κ than the original Callaway model and overestimates the κ.

In the earlier study [16,20,21,24–27], the Callaway model was always used along with Debye phonon dispersions and some parametrized relaxation times fitted with experiment data. Thus, we wonder whether the Callaway model and Allen's modified model can work better under similar approximated conditions. First, the linear phonon dispersions are used instead of the *ab initio* phonon dispersions. Only isotropic acoustic branches are considered in the actual BZ, and the three speeds of sound for the TA1, TA2, and LA branches are 12.0×10^3, 13.0×10^3, and 18.0×10^3 m/s, respectively, which are based on the values of diamond. Then, for the three-phonon transition rate determined by the corresponding matrix element $|V_{\lambda\lambda'\lambda''}|$ [36,40,54], the long wavelength approximation (LWA) for acoustic phonons is applied, i.e., $|V_{\lambda\lambda'\lambda''}| = C|q_\lambda||q_{\lambda'}||q_{\lambda''}|$ [37], where C is a scaling parameter. Although Ward and Broido [37] report the LWA holds for only a small fraction of the phase space of three-phonon scattering events, we apply it to the whole BZ. In order for the iteratively calculated κ under these approximations to be comparable with the accurate κ of diamond, we use $C^2 = 1.75 \times 10^{24}$ J^{-1} THz^6 nm^6, such that a less than 3% difference exists at room temperature. Figure 4 shows κ calculated from different models under these approximations. It can be seen that the original Callaway model and Allen's modified model still fail to predict κ correctly. For instance, the original Callaway model overestimates κ by about 26%, while Allen's modified model even overestimates by 108% at room temperature.

C. AlN

Thermal conductivity of wurtzite AlN can be characterized by its in-plane and cross-plane components. The anisotropy between the two components provides another degree of freedom to check the accuracy of the models. The calculated κ as a function of temperature is plotted in Fig. 5 for wurtzite AlN. For the in-plane κ of AlN, the accurate κ calculated iteratively is higher than RTA by 11% at room temperature. Above 150 K, while the original Callaway model has excellent correction, Allen's modified model overestimates κ by over 10%. However, at 100 K where the RTA underestimates by about 26%, the original Callaway model corrects worse

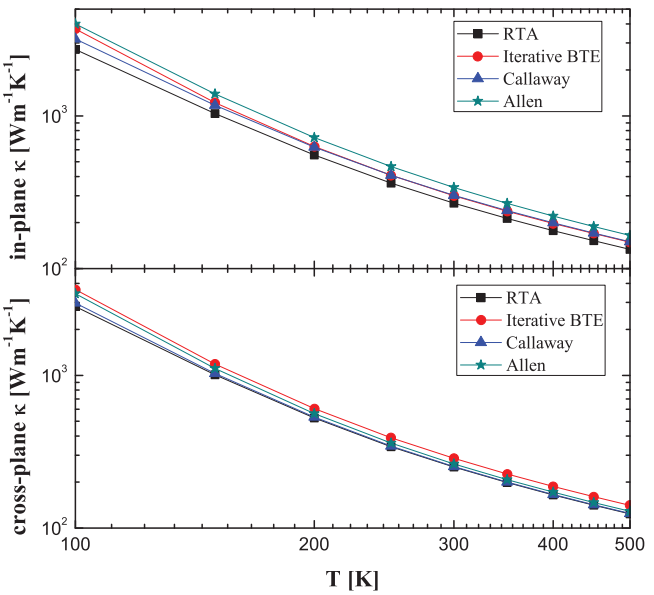

FIG. 5. (Color online) Thermal conductivity of wurtzite AlN calculated with different methods for solving phonon BTE, as a function of temperature. The top panel is for in-plane thermal conductivity and the bottom panel is for cross-plane thermal conductivity.

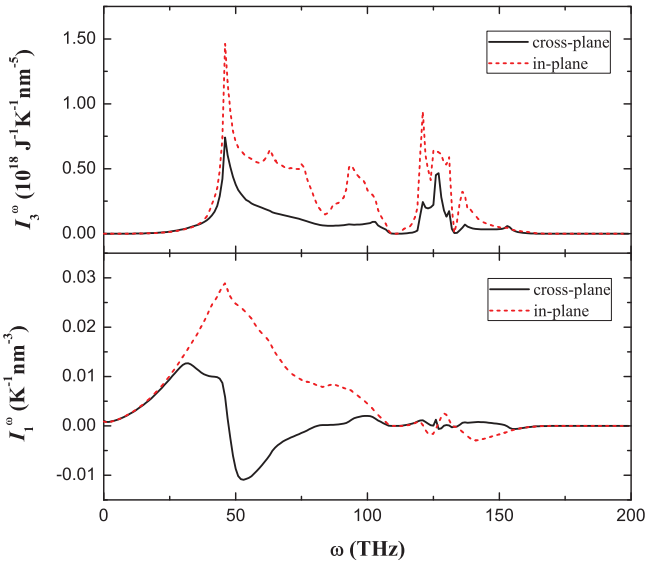

FIG. 6. (Color online) Frequency dependent contribution of the correction terms of the original Callaway model for wurtzite AlN. The top panel is for the I_3 term while the bottom panel is for the $I_1(=I_2)$ term.

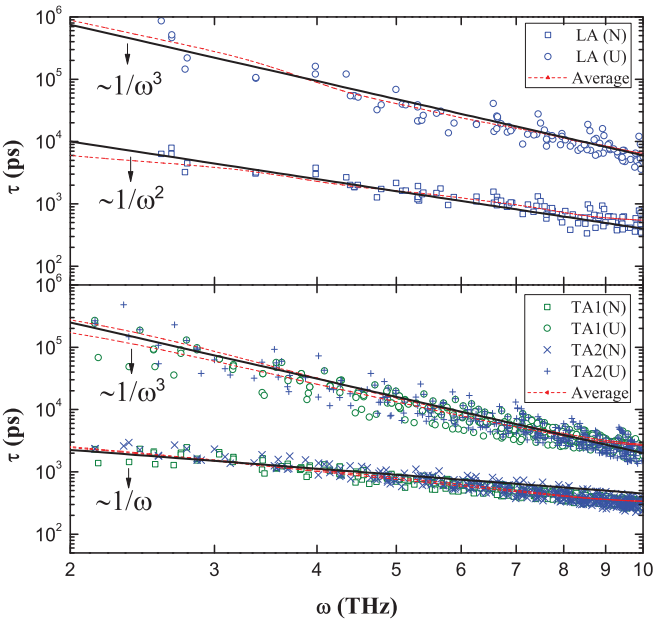

FIG. 7. (Color online) Relaxation time of N processes and U processes in wurtzite AlN at 300 K, as a function of frequency. The top panel is for the LA branch and the bottom panel is for the TA1 and TA2 branches. The discrete data are *ab initio* results, the dashed lines are the averaged relaxation times, and the solid lines are fitting lines.

than Allen's modified model, with deviations by 14% and 8%, respectively. The RTA, original Callaway model, and Allen's modified model underestimate the cross-plane κ. For instance, the underestimation of room temperature κ is 12.3%, 11.6%, and 8%, respectively. The original Callaway model only shows a 0.7% increase over RTA. Comparing the in-plane κ (300 W m^{-1} K^{-1}) and cross-plane κ (286 W m^{-1} K^{-1}) of AlN at room temperature, the anisotropy of wurtzite AlN is only 5%. However, because the Callaway model does not correctly predict the cross-plane κ, it gives a larger anisotropy than the actual value, and even that obtained from RTA in the temperature range considered here. To be specific, at room temperature, the RTA, Callaway model, and Allen's modified model obtain an anisotropy of 7% (268 vs 251 W m^{-1} K^{-1}), 19% (302 vs 253 m^{-1} K^{-1}), and 29% (340 vs 263 W m^{-1} K^{-1}), respectively, compared with the actual anisotropy of 5% (300 vs 286 W m^{-1} K^{-1}).

In order to figure out why the Callaway model gives a smaller correction to RTA for the cross-plane direction than for the in-plane direction, we plot the contribution from different frequencies to the correction terms I_1, I_2, and I_3 in the original Callaway model in Fig. 6. The top panel is for I_3 calculated with $I_3^\omega = \frac{1}{k_B T^2 NV} f_\lambda^0(1+f_\lambda^0)\sum_\lambda \frac{\tau_\lambda^c}{\tau_\lambda^N \tau_\lambda^U} q_\lambda^\alpha q_\lambda^\alpha \delta(\omega-\omega_\lambda)$. It is evident that I_3^ω is positive as it is related to the square of the wave vector. I_3^ω for the cross plane is smaller than that for the in plane, since the wave vectors have a shorter cross-plane component. Back to the correction terms of Eq. (13) ($\kappa = \kappa_{\rm RTA} + \frac{I_1 I_2}{I_3}$), even with smaller $I_3 = \int I_3^\omega d\omega$ for the cross-plane direction, the cross-plane correction value is still smaller. This reveals that I_1 and I_2 should be responsible for the smaller correction value obtained for the cross-plane direction. The contribution for $I_1(=I_2)$ calculated with $I_{1(2)}^\omega = \frac{\hbar\omega}{k_B T^2 NV} f_\lambda^0(1+f_\lambda^0)\sum_\lambda \frac{\tau_\lambda^c}{\tau_\lambda^N} v_\lambda^\alpha q_\lambda^\alpha \delta(\omega-\omega_\lambda)$ is plotted in the bottom panel of Fig. 6. It shows that $I_{1(2)}^\omega$ has a large range of negative values between 50 and 80 THz for the cross-plane direction while it is almost always positive for the in-plane direction, resulting in a much smaller $I_{1(2)} = \int I_{1(2)}^\omega d\omega$ for the cross-plane direction. The negative value comes from $v_\lambda^\alpha q_\lambda^\alpha$, which suggests there are many modes with negative $v_\lambda^\alpha q_\lambda^\alpha$ for the cross-plane direction between 50 and 80 THz.

Additionally, the frequency dependence of the relaxation time of wurtzite AlN is also discussed, as shown in Fig. 7. We calculate for $\omega < 10$ THz and use a $105 \times 105 \times 105$ mesh, where the results are converged for $\omega > 2$ THz. It can be seen that τ of the U processes for both LA and TA scales as $1/\omega^3$. τ^N scales as $1/\omega$ for TA, which is independent of lattice symmetry [63]. τ^N scales as $1/\omega^2$ for LA, in agreement with Herring's prediction about the hexagonal lattice structure [63]. To be specific, for the C_{6v} point group symmetry, which wurtzite AlN belongs to, as well as the D_{6h} and C_{6h} point groups, the LA branch obeys $1/\omega^2$ frequency dependence. For systems with D_6 and C_6 point group symmetries, these LA phonons exhibit $1/\omega^4$ dependence.

IV. CONCLUSIONS

In this paper, based on first principles calculation of phonon scatterings for Si, diamond, and wurtzite AlN, we examine the accuracy of the original Callaway model and Allen's modified version by comparing with an exact iterative solution of phonon BTE. Neither the original Callaway model nor Allen's modified model has guaranteed accuracy. In terms of relative error with respect to the accurate solution, the original Callaway model performs better than the ordinary RTA, while

Allen's modified version sometimes performs better than the original Callaway model or the ordinary RTA and sometimes worse. The anisotropy of AlN obtained from RTA is small, in agreement with the exact solution. However, both the Callaway model and Allen's modified version predict larger anisotropy. We have also studied the low frequency dependence of TA and LA relaxation times for these three systems. τ^U scale as $1/\omega^3$ for both TA and LA modes, and τ^N scales as $1/\omega$ and $1/\omega^2$ for TA and LA modes, respectively.

ACKNOWLEDGMENTS

We thank L. Lindsay, D. A. Broido, and D. A. Stewart for providing their *ab initio* interatomic force constants of silicon and diamond. We thank Natalio Mingo for helpful discussions on this work. J.L.M. and X.B.L. acknowledge support from National Nature Science Foundation of China (No. 51376070) and in part by the Major State Basic Research Development Program of China (No. 2011CB013105).

[1] R. E. Peierls, Ann. Phys. (Leipzig) **395**, 1055 (1929).
[2] J. M. Ziman, *Electrons and Phonons: The Theory of Transport Phenomena in Solids* (Oxford University Press, Oxford, U.K., 2001).
[3] J. Callaway, Phys. Rev. **113**, 1046 (1959).
[4] I. P. Morton and M. F. Lewis, Phys. Rev. B **3**, 552 (1971).
[5] H. E. Jackson and C. T. Walker, Phys. Rev. B **3**, 1428 (1971).
[6] C. R. Whitsett and D. A. Nelson, Phys. Rev. B **5**, 3125 (1972).
[7] C. R. Whitsett, D. A. Nelson, J. G. Broerman, and E. C. Paxhia, Phys. Rev. B **7**, 4625 (1973).
[8] J. E. Clemans, Phys. Rev. B **15**, 1072 (1977).
[9] T. J. Singh and G. S. Verma, Phys. Rev. B **19**, 1248 (1979).
[10] A. Noguera and S. M. Wasim, Phys. Rev. B **32**, 8046 (1985).
[11] K. C. Hass, M. A. Tamor, T. R. Anthony, and W. F. Banholzer, Phys. Rev. B **45**, 7171 (1992).
[12] Y.-J. Han and P. G. Klemens, Phys. Rev. B **48**, 6033 (1993).
[13] P. Stachowiak, V. V. Sumarokov, J. Mucha, and A. Jeżowski, Phys. Rev. B **50**, 543 (1994).
[14] J. E. Graebner, M. E. Reiss, L. Seibles, T. M. Hartnett, R. P. Miller, and C. J. Robinson, Phys. Rev. B **50**, 3702 (1994).
[15] M. Asen-Palmer, K. Bartkowski, E. Gmelin, M. Cardona, A. P. Zhernov, A. V. Inyushkin, A. Taldenkov, V. I. Ozhogin, K. M. Itoh, and E. E. Haller, Phys. Rev. B **56**, 9431 (1997).
[16] D. T. Morelli, J. P. Heremans, and G. A. Slack, Phys. Rev. B **66**, 195304 (2002).
[17] J. Zou, D. Kotchetkov, A. A. Balandin, D. I. Florescu, and F. H. Pollak, J. Appl. Phys. **92**, 2534 (2002).
[18] B. K. Singh, M. K. Roy, V. J. Menon, and K. C. Sood, Phys. Rev. B **67**, 014302 (2003).
[19] P. Stachowiak, V. V. Sumarokov, J. Mucha, and A. Jeżowski, Phys. Rev. B **67**, 172102 (2003).
[20] P. Stachowiak, V. V. Sumarokov, and A. Jeżowski, Phys. Rev. B **69**, 024305 (2004).
[21] W. Liu and A. A. Balandin, J. Appl. Phys. **97**, 073710 (2005).
[22] S. Barman and G. P. Srivastava, Phys. Rev. B **73**, 073301 (2006).
[23] W. Kim, J. Zide, A. Gossard, D. Klenov, S. Stemmer, A. Shakouri, and A. Majumdar, Phys. Rev. Lett. **96**, 045901 (2006).
[24] X. Lü and J. Chu, J. Appl. Phys. **101**, 114323 (2007).
[25] A. AlShaikhi and G. P. Srivastava, J. Appl. Phys. **103**, 083554 (2008).
[26] A. J. Minnich, H. Lee, X. W. Wang, G. Joshi, M. S. Dresselhaus, Z. F. Ren, G. Chen, and D. Vashaee, Phys. Rev. B **80**, 155327 (2009).
[27] A. AlShaikhi, S. Barman, and G. P. Srivastava, Phys. Rev. B **81**, 195320 (2010).
[28] M. Kazan, G. Guisbiers, S. Pereira, M. R. Correia, P. Masri, A. Bruyant, S. Volz, and P. Royer, J. Appl. Phys. **107**, 083503 (2010).
[29] Y. Zhang, E. Skoug, J. Cain, V. Ozoliņš, D. Morelli, and C. Wolverton, Phys. Rev. B **85**, 054306 (2012).
[30] A. Alofi and G. P. Srivastava, J. Appl. Phys. **112**, 013517 (2012).
[31] A. Alofi and G. P. Srivastava, Phys. Rev. B **87**, 115421 (2013).
[32] P. B. Allen, Phys. Rev. B **88**, 144302 (2013).
[33] M. Omini and A. Sparavigna, Physica B **212**, 101 (1995).
[34] M. Omini and A. Sparavigna, Phys. Rev. B **53**, 9064 (1996).
[35] M. Omini and A. Sparavigna, Nuovo Cimento Soc. Ital. Fis. D **19**, 1537 (1997).
[36] D. A. Broido, M. Malorny, G. Birner, N. Mingo, and D. A. Stewart, Appl. Phys. Lett. **91**, 231922 (2007).
[37] A. Ward and D. A. Broido, Phys. Rev. B **81**, 085205 (2010).
[38] K. Esfarjani, G. Chen, and H. T. Stokes, Phys. Rev. B **84**, 085204 (2011).
[39] A. Jain, Y.-J. Yu, and A. J. H. McGaughey, Phys. Rev. B **87**, 195301 (2013).
[40] A. Ward, D. A. Broido, D. A. Stewart, and G. Deinzer, Phys. Rev. B **80**, 125203 (2009).
[41] W. Li, N. Mingo, L. Lindsay, D. A. Broido, D. A. Stewart, and N. A. Katcho, Phys. Rev. B **85**, 195436 (2012).
[42] D. A. Broido, L. Lindsay, and A. Ward, Phys. Rev. B **86**, 115203 (2012).
[43] G. Fugallo, M. Lazzeri, L. Paulatto, and F. Mauri, Phys. Rev. B **88**, 045430 (2013).
[44] X. Tang and J. Dong, Proc. Natl. Acad. Sci. USA **107**, 4539 (2010).
[45] J. Garg, N. Bonini, B. Kozinsky, and N. Marzari, Phys. Rev. Lett. **106**, 045901 (2011).
[46] A. Kundu, N. Mingo, D. A. Broido, and D. A. Stewart, Phys. Rev. B **84**, 125426 (2011).
[47] W. Li and N. Mingo, J. Appl. Phys. **114**, 054307 (2013).
[48] J. Shiomi, K. Esfarjani, and G. Chen, Phys. Rev. B **84**, 104302 (2011).
[49] J. Carrete, W. Li, N. Mingo, S. Wang, and S. Curtarolo, Phys. Rev. X **4**, 011019 (2014).
[50] Z. Tian, J. Garg, K. Esfarjani, T. Shiga, J. Shiomi, and G. Chen, Phys. Rev. B **85**, 184303 (2012).
[51] L. Lindsay, D. A. Broido, and T. L. Reinecke, Phys. Rev. Lett. **109**, 095901 (2012).
[52] T. Luo, J. Garg, J. Shiomi, K. Esfarjani, and G. Chen, Europhys. Lett. **101**, 16001 (2013).
[53] L. Lindsay, D. A. Broido, and T. L. Reinecke, Phys. Rev. B **87**, 165201 (2013).
[54] W. Li, L. Lindsay, D. A. Broido, D. A. Stewart, and N. Mingo, Phys. Rev. B **86**, 174307 (2012).
[55] W. Li and N. Mingo, J. Appl. Phys. **114**, 183505 (2013).
[56] H. Dekura, T. Tsuchiya, and J. Tsuchiya, Phys. Rev. Lett. **110**, 025904 (2013).

[57] J. W. L. Pang, W. J. L. Buyers, A. Chernatynskiy, M. D. Lumsden, B. C. Larson, and S. R. Phillpot, Phys. Rev. Lett. **110**, 157401 (2013).
[58] L. Lindsay, D. A. Broido, and T. L. Reinecke, Phys. Rev. Lett. **111**, 025901 (2013).
[59] W. Li and N. Mingo, Phys. Rev. B **89**, 184304 (2014).
[60] W. Li, J. Carrete, N. A. Katcho, and N. Mingo, Comput. Phys. Commun. **185**, 1747 (2014).
[61] D. A. Broido, A. Ward, and N. Mingo, Phys. Rev. B **72**, 014308 (2005).
[62] A. Chernatynskiy and S. R. Phillpot, Phys. Rev. B **82**, 134301 (2010).
[63] C. Herring, Phys. Rev. **95**, 954 (1954).